JOURNAL OF BACTERIOLOGY, July 2010, p. 3279–3286 Vol. 192, No. 13
0021-9193/10/$12.00 doi:10.1128/JB.00230-10

Initiation of Decay of *Bacillus subtilis rpsO* mRNA by Endoribonuclease RNase Y▽

Shiyi Yao and David H. Bechhofer*

Department of Pharmacology and Systems Therapeutics, Box 1603, Mount Sinai School of Medicine of New York University, New York, New York 10029

Received 3 March 2010/Accepted 18 April 2010

***rpsO* mRNA, a small monocistronic mRNA that encodes ribosomal protein S15, was used to study aspects of mRNA decay initiation in *Bacillus subtilis*. Decay of *rpsO* mRNA in a panel of 3′-to-5′ exoribonuclease mutants was analyzed using a 5′-proximal oligonucleotide probe and a series of oligonucleotide probes that were complementary to overlapping sequences starting at the 3′ end. The results provided strong evidence that endonuclease cleavage in the body of the message, rather than degradation from the native 3′ end, is the rate-determining step for mRNA decay. Subsequent to endonuclease cleavage, the upstream products were degraded by polynucleotide phosphorylase (PNPase), and the downstream products were degraded by the 5′ exonuclease activity of RNase J1. The *rpsO* mRNA half-life was unchanged in a strain that had decreased RNase J1 activity and no RNase J2 activity, but it was 2.3-fold higher in a strain with decreased activity of RNase Y, a recently discovered RNase of *B. subtilis* encoded by the *ymdA* gene. Accumulation of full-length *rpsO* mRNA and its decay intermediates was analyzed using a construct in which the *rpsO* transcription unit was under control of a bacitracin-inducible promoter. The results were consistent with RNase Y-mediated initiation of decay. This is the first report of a specific mRNA whose stability is determined by RNase Y.**

The rate of decay of an mRNA is important for determining the level of gene expression. Studies on the mechanism of mRNA decay in *Escherichia coli* have progressed based on detailed knowledge of the RNases involved in the process and construction of RNase mutant strains. In a generally accepted model that applies to the turnover of many *E. coli* mRNAs, the 5′-end-dependent RNase E is responsible for the rate-determining endonuclease cleavage, which produces an upstream fragment that is subject to 3′-to-5′ exonucleolytic decay by RNase II and a downstream fragment that is subject to further RNase E endonucleolytic cleavage (5, 25). Recent studies have suggested that, in some cases, a preliminary step in RNase E binding is conversion of the native triphosphate 5′ end, which is a poor substrate for RNase E binding (23, 26, 40), to a monophosphate 5′ end by pyrophosphatase activity (4, 11). Degradation from the 3′ end can also occur, and this is dependent on the 3′ extending activity of poly(A) polymerase (17).

A similar level of understanding of the mechanism of mRNA decay has not been achieved for the model Gram-positive organism *Bacillus subtilis.* Sequence homologues of some of the *E. coli* enzymes that play major roles in mRNA decay [e.g., RNase E, RNase II, and poly(A) polymerase] cannot be identified in the *B. subtilis* genome. Nevertheless, studies on a number of mRNAs, some of which are constitutively or inducibly stable, have suggested that mRNA decay in *B. subtilis* also initiates from the 5′ end (9). *B. subtilis* polynucleotide phosphorylase (PNPase), encoded by the *pnpA* gene, plays a major role in 3′-to-5′ exonucleolytic degradation of decay intermediates (16, 32, 42). In addition to PNPase, three other *B. subtilis* 3′-to-5′ exoribonucleases, RNase PH, RNase R, and YhaM, can participate in mRNA decay (32). Recently, the role of the RNase J enzymes (19) in *B. subtilis* mRNA turnover has become apparent. While the RNase J enzymes were initially purified on the basis of their endoribonuclease activity, it was shown subsequently that the essential enzyme RNase J1 also has 5′-to-3′ exoribonuclease activity (29), which is inhibited by a 5′-triphosphate end (14, 15). RNase J1 has been shown to be involved in decay and processing of a number of specific RNAs (2, 6, 14, 19, 45), and a transcriptome analysis demonstrated that hundreds of mRNAs had increased half-lives in a strain that had reduced levels of RNase J1 and in which the nonessential enzyme RNase J2 was deleted (27).

Other endonucleases of *B. subtilis* that have been characterized to some extent are Bs-RNase III, RNase M5, RNase P, RNase Z, EndoA (8), and Mini-III (8, 37), none of which has been shown to be required for decay of an mRNA. Very recently, the product of the essential gene *ymdA* (21) was renamed RNase Y by Commichau and colleagues, based on its association with other RNA-processing enzymes and its apparent involvement in processing of the *gapA* operon mRNA (7). Shahbabian and colleagues showed that a strain in which RNase Y was depleted showed a significant increase in global mRNA half-life, suggesting that this enzyme plays a key role in mRNA turnover (38).

Previously, we used 5′-proximal oligonucleotide probes to analyze the steady-state decay pattern of a number of small monocistronic mRNAs by comparing the patterns detected by 5′-proximal probes in wild-type and *pnpA* strains (32). In each of seven cases, prominent decay intermediates were observed in the *pnpA* strain but not in the wild-type strain. One of the mRNAs was the *rpsO* mRNA, a 388-nucleotide (nt) mRNA that encodes ribosomal protein S15 (Fig. 1). The 3′ ends of the prominent *rpsO* decay intermediates detected in the *pnpA* strain were mapped to the downstream side of predicted RNA

* Corresponding author. Mailing address: Department of Pharmacology and Systems Therapeutics, Box 1603, Mount Sinai School of Medicine of New York University, New York, NY 10029. Phone: (212) 241-5628. Fax: (212) 996-7214. E-mail: david.bechhofer@mssm.edu.
▽ Published ahead of print on 23 April 2010.

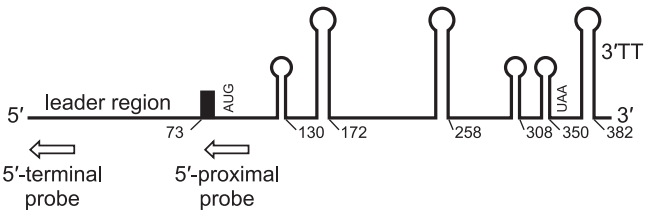

FIG. 1. Schematic diagram of the *rpsO* transcript, showing the locations of the Shine-Dalgarno sequence (filled rectangle), start and stop codons, five predicted stem-loop structures which appear to block 3′ exonuclease processivity (32), and 3′ transcription terminator (3′TT). The relative predicted strengths of the stem-loop structures are indicated roughly by the sizes of the stems. The locations of complementary probes used in Northern blot experiments to detect 5′-end-containing decay intermediates are also indicated.

structures. We suggested that the accumulation of these intermediates in the strains missing PNPase was the result of endonuclease cleavage downstream of the structure, followed by 3′-to-5′ exonuclease degradation up to the 3′ side of the structure. In strains containing PNPase, decay intermediates were not readily detected since PNPase could degrade RNA structures. In the current study, we used *rpsO* mRNA to obtain data supporting the endonucleolytic nature of decay initiation, and we obtained evidence that RNase Y is the decay-initiating endonuclease for *rpsO* mRNA.

MATERIALS AND METHODS

Bacterial strains. The triple and quadruple *B. subtilis* exoribonuclease mutant strains used in this study were derivatives of parent strain BG1 (*trpC2 thr-5*), which was designated the "wild-type" strain. Construction of exoribonuclease mutant strains has been described previously (32). The conditional endonuclease mutant strains used were RNase J1 (2), RNase P (43), RNase Z (33), and RNase Y (24) mutants. These strains contained plasmid pMAP65 (34), which provided additional copies of the *lac* repressor. *B. subtilis* strains were transformed as described previously (18).

***rpsO* transcription under p_{bac} control.** The p_{bac}-*rpsO* construct was assembled as follows. A 90-bp fragment of the *lia* operon promoter, including the LiaR binding sites (28), was amplified by PCR using an upstream oligonucleotide that included an MfeI restriction site. The *rpsO* transcriptional unit was amplified by PCR using an upstream primer that contained a 7-nt sequence complementary to the beginning of the downstream primer used for *lia* promoter region amplification and a downstream primer that included a HindIII site after the *rpsO* transcription terminator. The two PCR amplicons were annealed and were amplified using the 5′ *lia* promoter primer and the 3′ *rpsO* primer. The resulting product was digested with MfeI and HindIII and cloned into the EcoRI and HindIII sites of plasmid pDR67-Pm, a derivative of the *amyE* integration plasmid pDR67 (22) in which the chloramphenicol resistance gene is replaced by a phleomycin resistance gene (D. H. Bechhofer, unpublished data).

RNA analysis. RNA was isolated by hot phenol extraction from *B. subtilis* cultures grown in minimal medium containing Spizizen salts with 0.5% glucose, 0.1% Casamino Acids, 0.001% yeast extract, 50 μg/ml tryptophan, 50 μg/ml threonine, and 1 mM $MgSO_4$, as described previously (12). All strains were grown to the late logarithmic growth stage (100 Klett units, as determined using a no. 54 green filter), except for the quadruple 3′ exoribonuclease mutant, which was grown to a density of 50 Klett units. For the experiment whose results are shown in Fig. 3D, strains were grown in 2× YT medium containing 1% yeast extract, 2% tryptone, and 1% NaCl to an optical density at 600 nm (OD_{600}) of 0.6. Expression of RNase J1 and RNase Y in the conditional mutant strains was induced with 1 mM isopropyl-β-D-thiogalactopyranoside (IPTG). For induction of p_{bac} transcription, bacitracin was added to a final concentration of 50 μg/ml when strains had grown to a density of 75 Klett units. Northern blot analysis of RNA separated on 6% (see Fig. 2, 4, and 5) or 9% (see Fig. 3) denaturing polyacrylamide gels was performed as previously described (20). 5′-End-labeled oligonucleotide probes were prepared using T4 polynucleotide kinase and [γ-^{32}P]ATP. To control for RNA loading, membranes were stripped and probed for 5S rRNA, as described previously (39).

Data analysis. Quantitation of radioactivity in bands on Northern blots was performed with a Storm 860 PhosphorImager instrument (Molecular Dynamics) or a Typhoon TRIO variable-mode imager (GE Healthcare). The *rpsO* mRNA half-life was determined by a linear regression analysis of the percentage of RNA remaining versus time. Half-life data were obtained only from experiments in which the R^2 value was greater than 0.9. Wild-type and mutant RNA half-lives were compared using a two-sample *t* test to obtain *P* values. A *P* value of <0.05 was considered significant.

RESULTS

Half-life of *rpsO* mRNA in exonuclease mutants. Experiments were performed to determine whether the half-life of *rpsO* mRNA is affected by a deficiency of the known *B. subtilis* 3′-to-5′ exoribonucleases PNPase, RNase R, RNase PH, and YhaM. The chemical half-life of full-length *rpsO* mRNA was measured for strains that were deficient in three of the four exonucleases or in all four exonucleases. The reasoning was as follows. If decay was initiated by endonucleolytic cleavage, then the half-life of the full-length mRNA should not be affected by the absence of any of the known exonucleolytic activities. The effect of the exonuclease deficiency would be primarily on the fate of decay intermediates that are produced by endonuclease cleavage.

Total RNA was isolated from a *B. subtilis* wild-type strain and from exonuclease mutant strains at different times after addition of rifampin. Decay of *rpsO* mRNA was examined by Northern blot analysis, using a 5′-end-labeled oligonucleotide probe that was complementary to the translation initiation region (nt 75 to 100) of the *rpsO* message (5′-proximal probe) (Fig. 1). The Northern blots are shown in Fig. 2, and the half-life data are shown in Table 1. The half-life of *rpsO* mRNA in the wild-type strain was 3.2 min, and no prominent decay intermediates were detected (Fig. 2A). The *rpsO* mRNA half-life was slightly (but not significantly) longer (3.9 min) in the strain that contained PNPase but not the other three exoribonucleases (Table 1). As observed for the wild-type strain, prominent decay intermediates were not detected (Fig. 2B). We hypothesize that of the 3′ exonuclease activities present in *B. subtilis*, PNPase is the dominant activity and is able to degrade past strong secondary structures and eliminate decay intermediates (32). In the strain containing only RNase PH, many decay intermediates were detected, some of them in quantities that exceeded the amount of full-length mRNA (e.g., the "180-nt" RNA) (Fig. 2C), and these decay intermediates were stable throughout the course of the experiment. The same pattern was obtained when a 5′-terminal probe that was complementary to nt 1 to 24 of *rpsO* mRNA was used (Fig. 1) (data not shown). Thus, the 5′ end of these decay intermediates is likely to be at the transcription start site (TSS). Despite the massive accumulation of decay intermediates, the half-life of full-length *rpsO* mRNA in the strain containing only RNase PH was 4.3 min, which was not significantly different from the half-life in the strain containing only PNPase (Table 1). The strain that contained only YhaM showed a pattern of decay intermediates similar to that shown by the strain containing only RNase PH (Fig. 2D), and the half-life was longer (5.8 min) (Table 1). In the strain containing only RNase R, a slightly different pattern of decay intermediates was detected (Fig. 2E), but the half-life of full-length *rpsO* mRNA was also

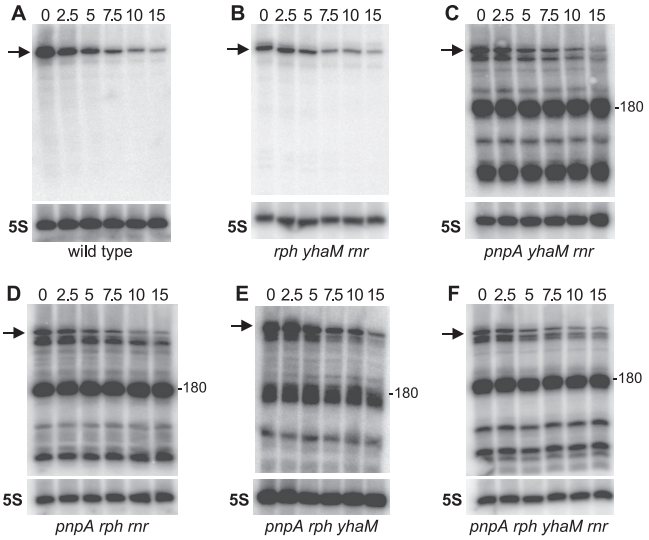

FIG. 2. Northern blot analysis of *rpsO* mRNA decay in 3′-to-5′ exoribonuclease mutants. The genotypes for the four known 3′ exoribonucleases are indicated below the panels. The numbers above the lanes are the times (in minutes) after rifampin addition. The probe was a 5′-end-labeled oligonucleotide complementary to the *rpsO* translation initiation region (nt 75 to 100) (Fig. 1). The position of full-length *rpsO* mRNA is indicated by the arrow on the left in each panel. The position of the prominent 180-nt decay intermediate is indicated on the right. The quantity of total RNA in each lane was corrected using the amount of RNA detected by a 5S rRNA-specific oligonucleotide probe, as shown at the bottom in each panel.

5.8 min. Finally, in the strain that was deficient for all four of the known 3′-to-5′ exoribonucleases, the half-life of full-length *rpsO* mRNA was 4.9 min (Fig. 2F and Table 1). The half-lives observed did not correlate with the previously measured doubling times of the mutant strains (32). For example, the quadruple mutant has a doubling time that is 1.5 to 2 times longer than the doubling times of the triple mutants, yet the *rpsO* mRNA half-life was shorter in the quadruple mutant. These results indicated that 3′ exonuclease activity has a minor role in determining the *rpsO* mRNA half-life. Endonuclease cleavage was presumably the major determinant of the mRNA half-life.

Decay intermediates containing the 3′ end. Endonuclease cleavage in the body of the *rpsO* message should generate upstream fragments containing the *rpsO* mRNA 5′ end (easily detected by the 5′-proximal probe in the PNPase-deficient mutants, as shown in Fig. 2) and downstream fragments containing the *rpsO* mRNA 3′ end. The stability of the downstream fragment should depend on its susceptibility to additional cleavage with endonucleases or to the 5′-to-3′ exonuclease activity of RNase J1. Presumably, the presence of the transcription terminator structure at the 3′ end of the downstream fragment protects against 3′-to-5′ exonucleolytic decay. We sought to detect such downstream fragments by using 11 overlapping oligonucleotide probes, each 36 nt long, that were complementary to sequences starting from the *rpsO* transcription terminator past the midpoint of the coding sequence (CDS) (Fig. 3A). These oligonucleotides were used in Northern blot analyses of RNA isolated from the wild-type strain (Fig. 3B). The blots were exposed for much longer times than those shown in Fig. 2. Figure 3B shows that fragments that contained the *rpsO* mRNA 3′ end could be detected, although the amounts were much smaller than the amounts of full-length mRNA. Multiple species were detected, and the clearest groups of bands were designated b to j, from the largest to the smallest (the full-length *rpsO* mRNA band was designated band "a"). From the data, it was clear that the 5′ ends of the smallest fragments were closest to the 3′ end of *rpsO* mRNA, since they could be detected only by the 3′-proximal probes. The 5′ ends of the larger fragments were located increasingly further upstream, since they could also be detected by probes complementary to sequences further upstream in the CDS. If we assume that comigrating bands observed with the different probes represent the same RNA fragments, then the patterns of the Northern blots demonstrated that all of the RNAs detected by the probes contained the 3′ end of *rpsO* mRNA. While there were not sufficient amounts of these RNAs to map their 5′ ends precisely, the extents of the RNA fragments could be approximated, based on size markers run in parallel and assuming that the fragments shared the same 3′ end. These fragments are shown schematically in Fig. 3A. Interestingly, the fragments appear to cluster in the 3′-proximal half of the transcript. We hypothesize that these RNA fragments resulted from one or more endonuclease cleavages downstream of the strong stem-loop near nt 180 and subsequent 5′-to-3′ processing. The fragments were detectable because they were protected by the transcription terminator structure, but, unlike the 5′-end-containing fragments (Fig. 2),

TABLE 1. RNase mutants and *rpsO* half-lives

Mutant type	RNase(s) present[a]	Exoribonuclease genotype[b]	*rpsO* half-life (min) (mean ± SD)[c]	*P* value[d]
Wild type	PNPase, RNase PH, YhaM, RNase R	NA[e]	3.24 ± 0.47	NA
Triple	PNPase	*rnr*::Tc *rph*ΩSp *yhaM*::Pm	3.94 ± 0.39	0.063
	RNase PH	*pnpA*::Cm *rnr*::Tc *yhaM*::Pm	4.30 ± 0.73	0.142
	YhaM	*pnpA*::Km *rnr*::Tc *rph*ΩSp	5.84 ± 0.82	0.035
	RNase R	*pnpA*::Km *rph*ΩSp *yhaM*::Pm	5.76 ± 0.65	0.025
Quadruple	None	*pnpA*::Cm *rnr*::Tc *rph*ΩSp *yhaM*::Pm	4.85 ± 0.15	<0.001

[a] The presence of the four known 3′-to-5′ exoribonucleases is indicated.
[b] The resistance markers were chloramphenicol (Cm), kanamycin (Km), phleomycin (Pm), spectinomycin (Sp), and tetracycline (Tc) resistance.
[c] The data are the results of three experiments.
[d] To determine *P* values, the half-lives for the mutant strains were compared to the half-life for the wild type.
[e] NA, not applicable.

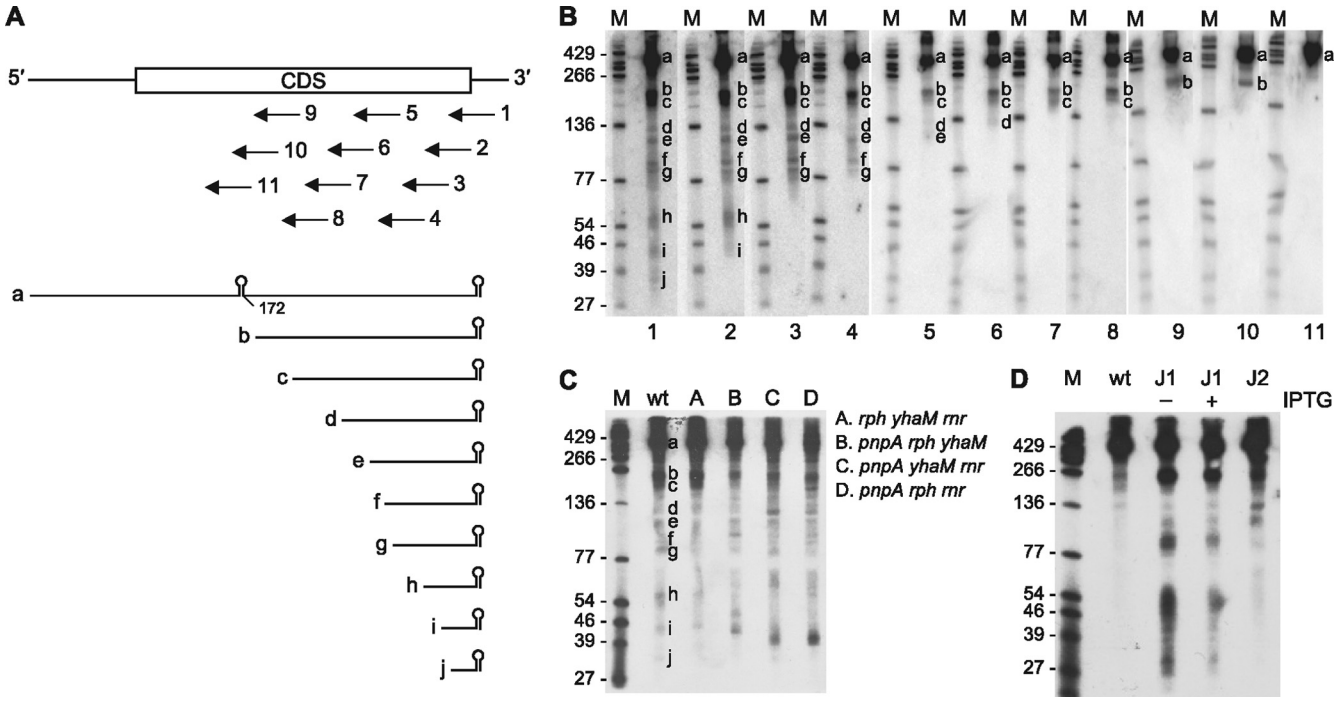

FIG. 3. Detection of 3′-end-containing mRNA decay fragments. (A) Linear diagram of *rpsO* transcript. The box representing the CDS corresponds to the interval between the AUG start codon and the UAA stop codon shown in Fig. 1. The region of complementarity for each of the 11 overlapping 3′-proximal probes (probes 1 to 11) used in the Northern blots in panel B is indicated. The approximate extents of 3′-end-containing mRNA decay fragments, designated using the letters used in panel B, are indicated below the probes. Fragment a is full-length *rpsO* mRNA, and the stem-loop that ends at nt 172 (see Fig. 1) and that gives rise to the "180-nt" decay intermediate is shown for reference. The diagrams for RNA fragments b to j represent not single RNAs but groups of RNAs with 5′ endpoints that are close to each other. (B) Northern blot analysis of 3′-end-containing *rpsO* decay fragments in the wild-type strain. The probe used is indicated below each blot. Groups of fragments are labeled b to j to the right of each lane containing total RNA. The marker lanes (lanes M) contained 5′-end-labeled fragments of a TaqI digest of plasmid pSE420 (3). The numbers on the left indicate molecular sizes (in nucleotides). (C) Northern blot analysis of 3′-end-containing fragments in triple RNase mutants, using probe 1. The wild type (wt) contained all four known 3′-to-5′ exoribonucleases. The genotypes for the four known 3′ exoribonucleases are indicated on the right. For an explanation of lane M see above. (D) Northern blot analysis of 3′-end-containing fragments in RNase J1 and RNase J2 mutant strains, using probe 1. The RNase J1 conditional mutant was grown in the presence (+) or absence (−) of IPTG, as indicated. For an explanation of lane M see above.

they were unstable because they were susceptible to further endonucleolytic or 5′ exonucleolytic attack.

Pattern of 3′-end-containing fragments in exoribonuclease mutants. A considerable difference in the pattern of 5′-end-containing decay intermediates was observed between strains that contained PNPase and strains that did not contain PNPase (Fig. 2, compare panels A and B and panels C to F). According to our model, these decay intermediates arose by endonuclease cleavage in the body of the message, followed by 3′-to-5′ exonucleolytic decay up to the 3′ side of RNA structures, which blocked 3′ exonucleases other than PNPase (32). On the other hand, we predicted that the pattern of 3′-end-containing decay fragments (Fig. 3B), which were the downstream fragments resulting from endonuclease cleavage, should not be affected significantly by the type of 3′ exonuclease activity present in the cell. This prediction was tested directly by performing a Northern blot analysis of 3′-end-containing fragments in the various triple exonuclease mutant strains, using 3′-terminal probe 1 (Fig. 3C). The results showed that the patterns of 3′-end-containing fragments in the wild-type and RNase mutant strains, although not identical, were similar in terms of the sizes and amounts of RNA fragments.

Levels of 3′-end-containing fragments in RNase J mutant strains. Although 3′-end-containing fragments were detectable in the wild-type strain, their abundance was relatively low. We tested whether RNase J1 or RNase J2 was responsible for degradation of these fragments by repeating the Northern blot analysis using probe 1 with RNA isolated from RNase J mutant strains. In the RNase J1 mutant strain *rnjA* expression is under the control of an IPTG-inducible promoter. When grown in the absence of IPTG, the RNase J1 mutant strain contains a much lower level of enzyme, while growth in the presence of IPTG results in a ~5-fold-lower level of enzyme (10). As Fig. 3D shows, the intensity of the steady-state pattern of small fragments in the RNase J1 mutant strain grown with IPTG was somewhat greater than that in the wild-type strain but the intensity was much greater when the organism was grown without IPTG. Deletion of the RNase J2 gene did not have a clear effect on the decay intermediate pattern. (In this experiment, the amount of full-length RNA in the RNase J2 mutant lane was about 20% greater than the amount in the wild-type lane. Hence, the lower bands in the RNase J2 mutant lane are more visible than those in the wild-type lane, but the patterns are the same.) We concluded that RNase J1 is

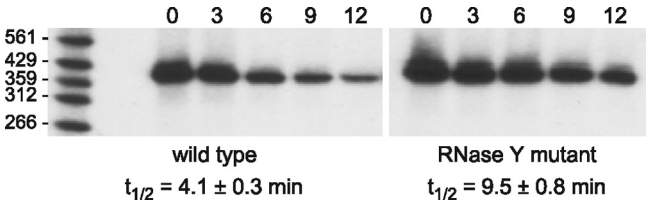

FIG. 4. Northern blot analysis of *rpsO* mRNA decay in wild-type and RNase Y mutant strains. The probe was the 5′-proximal probe (Fig. 1). The numbers above the lanes indicate the times (in minutes) after rifampin addition. The measured half-life ($t_{1/2}$) (average ± standard deviation of three experiments) is indicated below each blot. For an explanation of the marker lane on the left see the legend to Fig. 3.

responsible for turnover of the downstream fragments that arise by endonuclease cleavage.

***rpsO* mRNA half-life in endonuclease mutant strains.** At the time that this study of *rpsO* mRNA decay was begun, RNase J1 was the only endonuclease of *B. subtilis* known to be involved in initiation of mRNA decay. We thus thought that RNase J1 could be responsible for the endonucleolytic cleavage that was suggested by the analysis of *rpsO* mRNA decay intermediates. Northern blot analysis was used to measure the *rpsO* mRNA half-life in the RNase J1 conditional mutant strain grown in the presence of 1 mM IPTG. The decrease in the RNase J1 level in the conditional mutant strain, even when IPTG is present, is sufficient to detect changes in the half-lives of RNAs whose decay is RNase J1 dependent (10, 13, 44). We found, however, that the half-life of *rpsO* mRNA in the RNase J1 mutant was 3.9 min (data not shown), which is not significantly different from the 3.2-min half-life in the wild type. The half-life in an RNase J1 mutant strain in which the RNase J2 gene was deleted was similar (3.8 min). More recent reports have identified RNase Y as a potentially major player in RNA decay and processing in *B. subtilis* (see Discussion). We therefore measured the half-life of *rpsO* mRNA in the RNase Y conditional mutant grown in the presence of 1 mM IPTG. The growth rate of the RNase Y mutant strain under these conditions was only slightly lower than that of the wild type (data not shown). Northern blot analysis of *rpsO* mRNA decay in the wild-type and RNase Y mutant strains after addition of rifampin showed that there was a 2.3-fold increase in the mRNA half-life (Fig. 4).

System to monitor the appearance of decay intermediates over time. The prominent *rpsO* mRNA decay intermediates observed at steady state in the PNPase-deficient strains (Fig. 2) suggested that we could use an inducible system to follow accumulation of these fragments over time in order to confirm the involvement of a particular endonuclease in initiation of decay. Several problems were encountered when we performed time course analyses using the conventional IPTG-inducible or xylose-inducible promoters. First, since the *rpsO* 5′-end-containing decay intermediates were extremely stable (Fig. 2), we needed an inducible transcription system that was not "leaky," as ongoing low-level transcription in the absence of inducer would lead to steady-state accumulation of RNA fragments. The IPTG- and xylose-inducible systems, which are negatively regulated by repressors, were somewhat leaky (data not shown). Second, examination of the appearance of decay intermediates requires an induction system that scales up to full induction over a reasonably long period of time. We found that full induction occurred over an extremely short time period when IPTG- and xylose-inducible systems were used (data not shown). Third, regulation of the commonly used inducible promoters depends on the presence of an operator sequence located downstream of the TSS. This means that the induced transcript contains the cognate operator sequence, which gives a 5′-proximal sequence very different from the native transcript. This may be problematic for studying mRNA decay that could be 5′ end dependent.

To avoid some of these issues, we created a new inducible system that relies on the bacitracin-inducible promoter of the *lia* operon (28). This promoter is induced positively by subinhibitory concentrations of bacitracin, and we designated it the "p_{bac}" promoter. A 90-bp fragment encompasses the promoter and the upstream regulatory region at which the transcriptional activator, LiaR, binds when bacitracin is present (28). A construct in which the p_{bac} promoter fragment was located so that transcription started at the *rpsO* TSS was integrated at the *amyE* locus to obtain "p_{bac}-*rpsO* mRNA." To differentiate between native *rpsO* mRNA and p_{bac}-*rpsO* mRNA, nt 8 to 16 of the *rpsO* sequence (UAAAACCAU) were changed to the complementary sequence. *B. subtilis rpsO* mRNA begins with a leader region (Fig. 1), which includes a predicted pseudoknot structure (41) that is thought to be involved in translational autoregulation (35, 36). However, the pseudoknot structure begins at nt 30, and we assumed that changing nt 8 to 16 would not affect decay characteristics of the message. In these experiments, we used a bacitracin concentration of 50 μg/ml (equivalent to 3.5 U/ml), which results in full induction but does not significantly affect bacterial growth (31).

The results of a Northern blot analysis of the induction kinetics of p_{bac}-*rpsO* mRNA in the *pnpA* strain are shown in Fig. 5A. The probe was directed to the 5′ end of p_{bac}-*rpsO* mRNA. Before addition of bacitracin (Fig. 5A, lane B) no signal was detected, demonstrating that the probe does not detect native *rpsO* mRNA. The p_{bac}-*rpsO* mRNA was detected faintly at 1 min, and the level increased over time; almost full induction occurred at around 15 min (Fig. 5B). At this time, the prominent 180-nt decay intermediate was visible, suggesting that the nature of the promoter and the change in the 5′-proximal sequence do not affect mRNA processing.

Induction of p_{bac}-*rpsO* mRNA in endonuclease mutants. A time course analysis of the accumulation of full-length p_{bac}-*rpsO* mRNA and decay intermediates was performed using several endonuclease mutant backgrounds. There was no difference between the single-mutant *pnpA* strain and the *pnpA* strain that had decreased levels of RNase J1 and no RNase J2 (Fig. 5B). This finding correlated with the similar half-lives of *rpsO* in the wild-type and RNase J1 mutant strains, as described above. Similarly, the bacitracin-induced time course was not affected in strains with reduced levels of RNase P and RNase Z (data not shown). However, the results obtained with the RNase Y mutant strain were informative. At the earliest time point (0.5 min), p_{bac}-*rpsO* mRNA was virtually undetectable in the *pnpA* strain but was clearly present in the double mutant strain with reduced RNase Y (Fig. 5C). Over time, compared to full-length p_{bac}-*rpsO* mRNA, the amount of the 180-nt decay intermediate that accumulated increased much more in the *pnpA* strain than in the double-mutant strain with

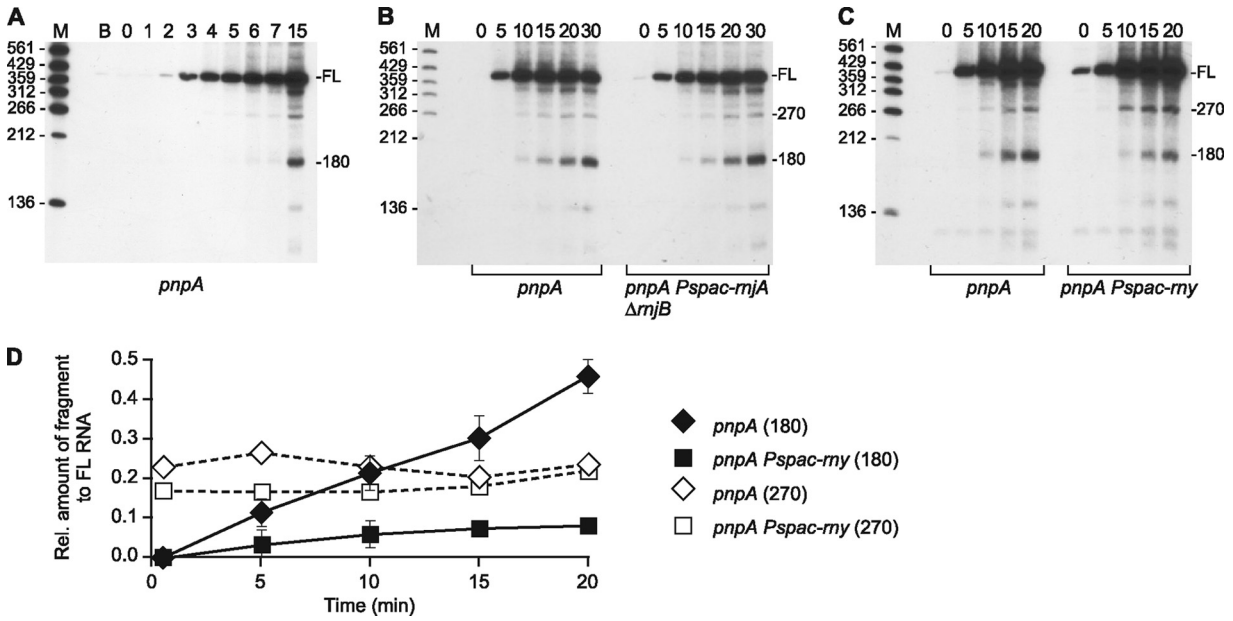

FIG. 5. Time course of p_{bac}-*rpsO* mRNA accumulation. (A) Induction of p_{bac}-*rpsO* transcription. The positions of full-length (FL) p_{bac}-*rpsO* and a prominent decay intermediate (180 nt) are indicated on the right. The numbers above the lanes indicate the times (in minutes) after addition of bacitracin. The "zero" time point in panels A to C is actually the interval between addition of bacitracin and removal and processing of the first aliquot, which was about 30 s. Lane B contained RNA isolated before addition of bacitracin. For an explanation of the marker lane (lane M) see the legend to Fig. 3. (B) Accumulation of decay intermediates in the *pnpA* strain and in the *pnpA* strain with a reduced level of RNase J1 and no RNase J2. (C) Appearance of decay intermediates in the *pnpA* strain and the *pnpA* strain with a reduced level of RNase Y. (D) Ratios of the 180-nt decay intermediate (solid lines) and the 270-nt decay intermediate (dashed lines) to full-length p_{bac}-*rpsO* in the *pnpA* strain (diamonds) and the *pnpA Pspac-rny* double mutant strain (squares). Error bars are shown only for the 180-nt decay intermediate. The RNase genotypes and fragment sizes (in nucleotides, in parentheses) are indicated on the right.

reduced RNase Y (Fig. 5D). These results are consistent with initiation of decay by RNase Y cleavage. One other prominent RNA, which was about 270 nt long, was detected, but quantitative analysis of this RNA showed that it did not accumulate compared to the full-length RNA (Fig. 5D).

DISCUSSION

The analysis of *rpsO* mRNA half-life in 3′ exonuclease mutants (Table 1 and Fig. 2) indicated that 3′-to-5′ exoribonucleases have a minor role in determining this mRNA half-life. We observed slight but not statistically significant increases in the *rpsO* mRNA half-life in strains containing only PNPase or only RNase PH and <2-fold increases in the *rpsO* mRNA half-life in strains containing only YhaM, only RNase R, or none of the known 3′ exonucleases. These results suggested that 3′ exonucleases have some effect on the half-life of full-length *rpsO* mRNA, but endonuclease cleavage was likely more important for initiation of decay. We have no good explanation at present for the greater increase in the *rpsO* mRNA half-life in the strains containing only YhaM or RNase R, especially since the increase was greater than that in the strain containing none of the four known exoribonucleases (Table 1). Perhaps particular perturbations in the exoribonuclease complement of the cell indirectly affect endoribonuclease activity; recent evidence for a putative *B. subtilis* degradosome complex that includes PNPase, RNase J1, and RNase Y (7) may be indicative of other interactions between RNases.

Endonuclease cleavage in the *rpsO* mRNA decay pathway was also inferred from the detection of multiple RNA fragments that were different sizes but all contained the 3′ end (Fig. 3B). We found that the patterns were similar for the wild-type and exoribonuclease mutant strains examined (Fig. 3C), despite the enormous differences between these strains when the patterns detected with the 5′-proximal probe were examined (Fig. 2). The contrast between the complete lack of 5′-proximal decay intermediates in the strain containing only PNPase (Fig. 2B) and the presence of 3′-proximal decay intermediates in the same strain (Fig. 3C, lane A) is particularly striking and is consistent with initiation of decay by endonuclease cleavage. The 3′-terminal fragments may be direct products of endonuclease cleavage, or they may be secondary products of RNase J1 5′ exonuclease activity that proceeds from the 5′ end(s) generated by endonuclease cleavage. The low level of 3′-end-containing fragments in the wild-type strain likely occurs because RNase J1 is capable of degrading through the secondary structure in the 5′-to-3′ direction (14). Indeed, depleting the cell severely (without IPTG) or moderately (with IPTG) of RNase J1 resulted in increased intensity of the 3′-end-containing decay intermediates (Fig. 3D).

We found in assays of mRNA half-lives and of accumulation of full-length RNA and decay intermediates that RNase J1 was not responsible for determining the stability of *rpsO* mRNA. Although RNase Y, the product of the *ymdA* gene, was suspected long ago of being an RNase (1, 9), only in the last year have data on the role of RNase Y in RNA processing been described. Meinken and colleagues obtained evidence that cleavage of *gapA* operon mRNA at a particular site (30) was

due to RNase Y (7). Shahbabian and colleagues demonstrated that cleavage of the *yitJ* riboswitch RNA, as well as other *S*-adenosylmethionine-dependent riboswitches, could be attributed to RNase Y (38). They also found that depletion of RNase Y resulted in an increase in the half-life of bulk mRNA. Thus, we turned our attention to RNase Y and showed, for the first time, that RNase Y has an effect on decay of a specific *B. subtilis* mRNA. We observed a >2-fold increase in the *rpsO* mRNA half-life in the RNase Y conditional mutant (Fig. 4). This suggests that there is a strong dependence on RNase Y for initiation of decay, since we assumed that the RNase Y conditional mutant grown with 1 mM IPTG contains a significant level of the enzyme. We have not proven that RNase Y acts directly on *rpsO* mRNA, which would require *in vitro* tests, and it is possible that a deficiency in RNase Y has indirect effects on initiation of mRNA decay. Nevertheless, the simplest interpretation of our results is that RNase Y cleaves *rpsO* mRNA, and for the discussion below we assume that this is the case.

The p_{bac} system was useful for demonstrating faster accumulation of full-length *rpsO* mRNA in the RNase Y mutant strain (Fig. 5C, zero-time lane), presumably because initiation of decay was slower due to the lower level of RNase Y. We hypothesize that the 180-nt RNA results from endonuclease cleavage followed by 3′ exonuclease activity up to the strong stem-loop structure that ends at nt 172. Thus, if RNase Y cleavage is required to generate this RNA, accumulation of the RNA should be slower in the RNase Y mutant, and this was indeed the case (Fig. 5C and 5D). Other bands, in addition to the full-length and 180-nt bands, were detected (Fig. 5C). Some of these bands were faint and were present throughout the time course, and these bands likely represent nonspecific hybridization. We speculate that the band at around 270 nt may be a prematurely terminated transcription product or a processing product of a different RNase acting on full-length RNA.

From the current analysis of *rpsO* mRNA decay intermediates, it was not clear if RNase Y cleaves once or several times in the body of the message. Even a single endonuclease cleavage could give rise to numerous decay intermediates due to subsequent 3′-to-5′ exonuclease and 5′-to-3′ exonuclease activities and hindrance of these activities by RNA structure. In any event, the results obtained to date allow construction of a preliminary model for the complete turnover of *rpsO* mRNA, which begins with endonuclease cleavage by RNase Y and is completed by the 3′ exonuclease activity of PNPase on upstream products and the 5′ exonuclease activity of RNase J1 on downstream products (Fig. 6). As RNase Y is essential, we expect that RNase Y catalyzes decay-initiating cleavage of many *B. subtilis* mRNAs.

Unlike RNase J1, which has robust endonuclease activity with 5′ triphosphorylated substrates (14, 15), RNase Y endonuclease activity is sensitive to the nature of the 5′ end, and the *in vitro* activity on RNA with a 5′ monophosphorylated end is significantly higher (38). If this is also true of RNase Y activity *in vivo*, it has major consequences for models of RNase Y-dependent initiation of decay. Figure 2 shows that decay intermediates detected in the PNPase-deficient strains were extremely stable, and their intensities did not decrease throughout the experiment. This suggests that degradation by

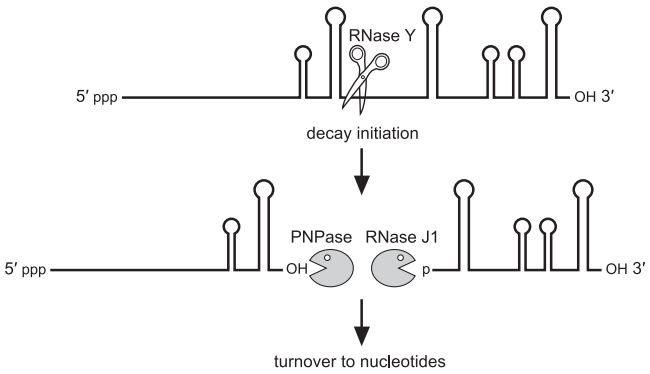

FIG. 6. Model for the pathway of *rpsO* mRNA decay. Only a single RNase Y endonuclease cleavage site is shown, but there may be additional cleavage sites.

RNase J1 5′ exonucleolytic activity from the native 5′ end did not occur, even though the data in Fig. 3D indicate that the same 5′ exonuclease activity degraded the 3′-end-containing fragments. This suggests that the 5′ triphosphate group of the initial *rpsO* transcription product is not removed, making 5′-end-containing decay intermediates resistant to RNase J1 5′ exonucleolytic decay. However, if this is the case and if RNase Y is sensitive to the 5′ triphosphate end, then it is hard to understand how internal cleavage by RNase Y resulting in a relatively short half-life (3.2 min) occurs. Much work is needed to understand the basis of endonucleolytic cleavage by RNase J1 and RNase Y and to determine why particular messages are subject to one of the activities or perhaps both activities.

ACKNOWLEDGMENT

This work was supported by Public Health Service grant GM-48804 from the National Institutes of Health to D.H.B.

REFERENCES

1. **Aravind, L., and E. V. Koonin.** 2001. A natural classification of ribonucleases. Methods Enzymol. **341:**3–28.
2. **Britton, R. A., T. Wen, L. Schaefer, O. Pellegrini, W. C. Uicker, N. Mathy, C. Tobin, R. Daou, J. Szyk, and C. Condon.** 2007. Maturation of the 5′ end of Bacillus subtilis 16S rRNA by the essential ribonuclease YkqC/RNase J1. Mol. Microbiol. **63:**127–138.
3. **Brosius, J.** 1992. Compilation of superlinker vectors. Methods Enzymol. **216:**469–483.
4. **Celesnik, H., A. Deana, and J. G. Belasco.** 2007. Initiation of RNA decay in Escherichia coli by 5′ pyrophosphate removal. Mol. Cell **27:**79–90.
5. **Coburn, G. A., and G. A. Mackie.** 1999. Degradation of mRNA in Escherichia coli: an old problem with some new twists. Prog. Nucleic Acid Res. Mol. Biol. **62:**55–5108.
6. **Collins, J. A., I. Irnov, S. Baker, and W. C. Winkler.** 2007. Mechanism of mRNA destabilization by the glmS ribozyme. Genes Dev. **21:**3356–3368.
7. **Commichau, F. M., F. M. Rothe, C. Herzberg, E. Wagner, D. Hellwig, M. Lehnik-Habrink, E. Hammer, U. Volker, and J. Stulke.** 2009. Novel activities of glycolytic enzymes in Bacillus subtilis: interactions with essential proteins involved in mRNA processing. Mol. Cell. Proteomics **8:**1350–1360.
8. **Condon, C.** 2007. Maturation and degradation of RNA in bacteria. Curr. Opin. Microbiol. **10:**271–278.
9. **Condon, C.** 2003. RNA processing and degradation in Bacillus subtilis. Microbiol. Mol. Biol. Rev. **67:**157–174.
10. **Daou-Chabo, R., N. Mathy, L. Benard, and C. Condon.** 2009. Ribosomes initiating translation of the hbs mRNA protect it from 5′-to-3′ exoribonucleolytic degradation by RNase J1. Mol. Microbiol. **71:**1538–1550.
11. **Deana, A., H. Celesnik, and J. G. Belasco.** 2008. The bacterial enzyme RppH triggers messenger RNA degradation by 5′ pyrophosphate removal. Nature **451:**355–358.
12. **Deikus, G., P. Babitzke, and D. H. Bechhofer.** 2004. Recycling of a regulatory protein by degradation of the RNA to which it binds. Proc. Natl. Acad. Sci. U. S. A. **101:**2747–2751.

13. **Deikus, G., and D. H. Bechhofer.** 2007. Initiation of decay of Bacillus subtilis trp leader RNA. J. Biol. Chem. **282:**20238–20244.
14. **Deikus, G., C. Condon, and D. H. Bechhofer.** 2008. Role of Bacillus subtilis RNase J1 endonuclease and 5′-exonuclease activities in trp leader RNA turnover. J. Biol. Chem. **283:**17158–17167.
15. **de la Sierra-Gallay, I. L., L. Zig, A. Jamalli, and H. Putzer.** 2008. Structural insights into the dual activity of RNase J. Nat. Struct. Mol. Biol. **15:**206–212.
16. **Deutscher, M. P., and N. B. Reuven.** 1991. Enzymatic basis for hydrolytic versus phosphorolytic mRNA degradation in Escherichia coli and Bacillus subtilis. Proc. Natl. Acad. Sci. U. S. A. **88:**3277–3280.
17. **Dreyfus, M., and P. Regnier.** 2002. The poly(A) tail of mRNAs: bodyguard in eukaryotes, scavenger in bacteria. Cell **111:**611–613.
18. **Dubnau, D., and R. Davidoff-Abelson.** 1971. Fate of transforming DNA following uptake by competent Bacillus subtilis. I. Formation and properties of the donor-recipient complex. J. Mol. Biol. **56:**209–221.
19. **Even, S., O. Pellegrini, L. Zig, V. Labas, J. Vinh, D. Brechemmier-Baey, and H. Putzer.** 2005. Ribonucleases J1 and J2: two novel endoribonucleases in B. subtilis with functional homology to E. coli RNase E. Nucleic Acids Res. **33:**2141–2152.
20. **Farr, G. A., I. A. Oussenko, and D. H. Bechhofer.** 1999. Protection against 3′-to-5′ RNA decay in Bacillus subtilis. J. Bacteriol. **181:**7323–7330.
21. **Hunt, A., J. P. Rawlins, H. B. Thomaides, and J. Errington.** 2006. Functional analysis of 11 putative essential genes in Bacillus subtilis. Microbiology **152:**2895–2907.
22. **Ireton, K., D. Z. Rudner, K. J. Siranosian, and A. D. Grossman.** 1993. Integration of multiple developmental signals in Bacillus subtilis through the Spo0A transcription factor. Genes Dev. **7:**283–294.
23. **Jiang, X., and J. G. Belasco.** 2004. Catalytic activation of multimeric RNase E and RNase G by 5′-monophosphorylated RNA. Proc. Natl. Acad. Sci. U. S. A. **101:**9211–9216.
24. **Kobayashi, K., S. D. Ehrlich, A. Albertini, G. Amati, K. K. Andersen, M. Arnaud, K. Asai, S. Ashikaga, S. Aymerich, P. Bessieres, F. Boland, S. C. Brignell, S. Bron, K. Bunai, J. Chapuis, L. C. Christiansen, A. Danchin, M. Debarbouille, E. Dervyn, E. Deuerling, K. Devine, S. K. Devine, O. Dreesen, J. Errington, S. Fillinger, S. J. Foster, Y. Fujita, A. Galizzi, R. Gardan, C. Eschevins, T. Fukushima, K. Haga, C. R. Harwood, M. Hecker, D. Hosoya, M. F. Hullo, H. Kakeshita, D. Karamata, Y. Kasahara, F. Kawamura, K. Koga, P. Koski, R. Kuwana, D. Imamura, M. Ishimaru, S. Ishikawa, I. Ishio, D. Le Coq, A. Masson, C. Mauel, R. Meima, R. P. Mellado, A. Moir, S. Moriya, E. Nagakawa, H. Nanamiya, S. Nakai, P. Nygaard, M. Ogura, T. Ohanan, M. O'Reilly, M. O'Rourke, Z. Pragai, H. M. Pooley, G. Rapoport, J. P. Rawlins, L. A. Rivas, C. Rivolta, A. Sadaie, Y. Sadaie, M. Sarvas, T. Sato, H. H. Saxild, E. Scanlan, W. Schumann, J. F. Seegers, J. Sekiguchi, A. Sekowska, S. J. Seror, M. Simon, P. Stragier, R. Studer, H. Takamatsu, T. Tanaka, M. Takeuchi, H. B. Thomaides, V. Vagner, J. M. van Dijl, K. Watabe, A. Wipat, H. Yamamoto, M. Yamamoto, Y. Yamamoto, K. Yamane, K. Yata, K. Yoshida, H. Yoshikawa, U. Zuber, and N. Ogasawara.** 2003. Essential Bacillus subtilis genes. Proc. Natl. Acad. Sci. U. S. A. **100:**4678–4683.
25. **Kushner, S. R.** 2002. mRNA decay in Escherichia coli comes of age. J. Bacteriol. **184:**4658–4665.
26. **Mackie, G. A.** 1998. Ribonuclease E is a 5′-end-dependent endonuclease. Nature **395:**720–723.
27. **Mader, U., L. Zig, J. Kretschmer, G. Homuth, and H. Putzer.** 2008. mRNA processing by RNases J1 and J2 affects Bacillus subtilis gene expression on a global scale. Mol. Microbiol. **70:**183–196.
28. **Mascher, T., S. L. Zimmer, T. A. Smith, and J. D. Helmann.** 2004. Antibiotic-inducible promoter regulated by the cell envelope stress-sensing two-component system LiaRS of Bacillus subtilis. Antimicrob. Agents Chemother. **48:**2888–2896.
29. **Mathy, N., L. Benard, O. Pellegrini, R. Daou, T. Wen, and C. Condon.** 2007. 5′-To-3′ exoribonuclease activity in bacteria: role of RNase J1 in rRNA maturation and 5′ stability of mRNA. Cell **129:**681–692.
30. **Meinken, C., H. M. Blencke, H. Ludwig, and J. Stulke.** 2003. Expression of the glycolytic gapA operon in Bacillus subtilis: differential syntheses of proteins encoded by the operon. Microbiology **149:**751–761.
31. **Ohki, R., K. Tateno, Y. Okada, H. Okajima, K. Asai, Y. Sadaie, M. Murata, and T. Aiso.** 2003. A bacitracin-resistant Bacillus subtilis gene encodes a homologue of the membrane-spanning subunit of the Bacillus licheniformis ABC transporter. J. Bacteriol. **185:**51–59.
32. **Oussenko, I. A., T. Abe, H. Ujiie, A. Muto, and D. H. Bechhofer.** 2005. Participation of 3′-to-5′ exoribonucleases in the turnover of Bacillus subtilis mRNA. J. Bacteriol. **187:**2758–2767.
33. **Pellegrini, O., J. Nezzar, A. Marchfelder, H. Putzer, and C. Condon.** 2003. Endonucleolytic processing of CCA-less tRNA precursors by RNase Z in Bacillus subtilis. EMBO J. **22:**4534–4543.
34. **Petit, M. A., E. Dervyn, M. Rose, K. D. Entian, S. McGovern, S. D. Ehrlich, and C. Bruand.** 1998. PcrA is an essential DNA helicase of Bacillus subtilis fulfilling functions both in repair and rolling-circle replication. Mol. Microbiol. **29:**261–273.
35. **Philippe, C., L. Benard, C. Portier, E. Westhof, B. Ehresmann, and C. Ehresmann.** 1995. Molecular dissection of the pseudoknot governing the translational regulation of Escherichia coli ribosomal protein S15. Nucleic Acids Res. **23:**18–28.
36. **Portier, C., L. Dondon, and M. Grunberg-Manago.** 1990. Translational autocontrol of the Escherichia coli ribosomal protein S15. J. Mol. Biol. **211:**407–414.
37. **Redko, Y., D. H. Bechhofer, and C. Condon.** 2008. Mini-III, an unusual member of the RNase III family of enzymes, catalyses 23S ribosomal RNA maturation in B. subtilis. Mol. Microbiol. **68:**1096–1106.
38. **Shahbabian, K., A. Jamalli, L. Zig, and H. Putzer.** 2009. RNase Y, a novel endoribonuclease, initiates riboswitch turnover in Bacillus subtilis. EMBO J. **28:**3523–3533.
39. **Sharp, J. S., and D. H. Bechhofer.** 2003. Effect of translational signals on mRNA decay in Bacillus subtilis. J. Bacteriol. **185:**5372–5379.
40. **Spickler, C., V. Stronge, and G. A. Mackie.** 2001. Preferential cleavage of degradative intermediates of rpsT mRNA by the Escherichia coli RNA degradosome. J. Bacteriol. **183:**1106–1109.
41. **Vitreshchak, A., A. K. Bansal, I. I. Titov, and M. S. Gel'fand.** 1999. Computer analysis of regulatory signals in complete bacterial genomes. Translation initiation of ribosomal protein operons. Biofizika **44:**601–610. (In Russian.)
42. **Wang, W., and D. H. Bechhofer.** 1996. Properties of a Bacillus subtilis polynucleotide phosphorylase deletion strain. J. Bacteriol. **178:**2375–2382.
43. **Wegscheid, B., C. Condon, and R. K. Hartmann.** 2006. Type A and B RNase P RNAs are interchangeable in vivo despite substantial biophysical differences. EMBO Rep. **7:**411–417.
44. **Yao, S., J. S. Sharp, and D. H. Bechhofer.** 2009. Bacillus subtilis RNase J1 endonuclease and 5′ exonuclease activities in the turnover of ΔermC mRNA. RNA **15:**2231–2339.
45. **Yao, S., J. B. Blaustein, and D. H. Bechhofer.** 2007. Processing of Bacillus subtilis small cytoplasmic RNA: evidence for an additional endonuclease cleavage site. Nucleic Acids Res. **35:**4464–4473.